ICIC Express Letters ICIC International ©2017 ISSN 1881-803X
Volume **11**, Number **3**, March **2017** pp. **665–671**

NONLINEAR CONTROL OF THREE-PHASE BOOST RECTIFIER BASED ON STATE ERROR HAMILTONIAN SYSTEMS

Haisheng Yu, Jinpeng Yu, Yu Gu and Peijie Hu

College of Automation and Electrical Engineering
Qingdao University
No. 308, Ningxia Road, Qingdao 266071, P. R. China
yu.hs@163.com

Received August 2016; accepted November 2016

Abstract. *The output direct current (DC) voltage control and power factor regulation of three-phase boost rectifiers are developed based on the state error port-controlled Hamiltonian (PCH) system. First of all, the PCH model is established for the rectifier. Then, a desired state error PCH structure is assigned to the closed-loop control system of the rectifier. The desired Hamiltonian function is given based on the energy-shaping. The controller is designed through interconnection assignment and damping injection. The feedback control problem is reduced to the solution of the partial differential equations. Moreover, a proportional integral (PI) regulation is used to eliminate the steady-state error of the output DC voltage. Consequently, the zero reactive current and unity power factor are achieved for the rectifier. Finally, compared with the conventional voltage-oriented control, the proposed control method has good dynamic and steady state performances. Simulation results illustrate the effectiveness of the proposed controller.*
Keywords: Nonlinear control, Rectifier, State error, Hamiltonian systems, Energy-shaping

1. **Introduction.** The three-phase pulse-width modulated (PWM) rectifiers are viewed as green power electronic equipments which possess attractive features such as nearly sinusoidal input current and unity power factor [1]. The traditional control strategies, for instance, voltage-oriented control (VOC) [2], current control [3], and direct power control [4] have been successfully applied to control of the PWM rectifiers.

With the development of advanced control methods, such as prediction control [5], without current sensors method [6], and adaptive control [7] they have been developed for three-phase boost rectifiers. In recent years, energy-shaping (ES) and port-controlled Hamiltonian (PCH) system control have attracted lots of attention [8,9]. The three-phase boost rectifiers are typical unity of energy and signal conversion. Applying energy-shaping and space vector PWM (SVPWM) technology, the PCH control methods of the motors have been studied [10-12]. In this paper, the output direct current (DC) voltage control and unity power factor regulation of three-phase boost rectifiers are developed based on the state error PCH system principle. The feedback control problem is reduced to the solution of a partial differential equation (PDE). In order to eliminate the steady-state error of the output DC voltage, the proportional integral (PI) control is also added to the system.

The paper is organized as follows. Section 2 presents the PCH model of three-phase boost rectifier. Section 3 develops the control of three-phase boost rectifier and describes the SVPWM implementation of the controller. Section 4 shows the comparative studies and simulation experiment results. At last, some conclusions are given.

2. **The PCH Model of Three-Phase Boost Rectifier.** The port-controlled Hamiltonian systems can be expressed as [8]

$$\dot{x} = [J(x,\mu) - R(x)]\frac{\partial H(x)}{\partial x} + g(x)u \tag{1}$$

where x is state vector, u is input vector and μ is the PWM duty ratio function of the rectifier. The matrix $R(x) = R^T(x) \geq 0$ represents the dissipation and matrix $J(x,\mu) = -J^T(x,\mu)$ represents interconnection structure. The matrix $g(x)$ is input function and $H(x)$ is Hamiltonian function.

The three-phase boost rectifier topology is shown in Figure 1, where $e_a = E_m \sin(\omega t)$, $e_b = E_m \sin\left(\omega t - \frac{2}{3}\pi\right)$ and $e_c = E_m \sin(\omega t + \frac{2}{3}\pi)$ are input voltages, C is the DC-side filter capacitor, r and L denote the resistance and inductance, respectively, and R_L is the resistive load. The switching functions $s_i = s_i(t) \in \{0,1\}$ $(i = a,b,c)$.

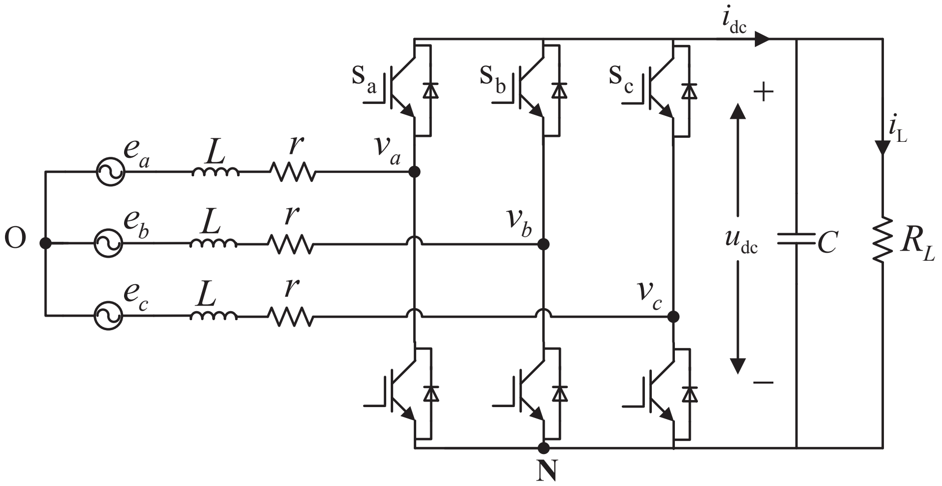

FIGURE 1. The main circuit schematic diagram

The mathematical model of the PWM rectifier in the d-q synchronously rotating reference frame can be expressed as [1]

$$\begin{cases} L\dfrac{di_d}{d_t} = e_d - ri_d + \omega L i_q - \mu_d u_{dc} \\ L\dfrac{di_q}{d_t} = e_q - ri_q - \omega L i_d - \mu_q u_{dc} \\ C\dfrac{du_{dc}}{d_t} = (\mu_d i_d + \mu_q i_q) - \dfrac{u_{dc}}{R_L} \end{cases} \tag{2}$$

where μ_d and μ_q are the duty ratio functions, $e_d = \sqrt{\frac{3}{2}}E_m$, and $e_q = 0$.

The state vector and input vector are defined as

$$x = \begin{bmatrix} x_1 & x_2 & x_3 \end{bmatrix}^T = \begin{bmatrix} Li_d & Li_q & Cu_{dc} \end{bmatrix}^T, \quad u = \begin{bmatrix} e_d & e_q \end{bmatrix}^T \tag{3}$$

Hamiltonian function is given by

$$H(x) = \frac{1}{2}x^T D^{-1} x, \quad D = diag(L, L, C) \tag{4}$$

Then the system (2) can be written in the form of system (1), that is

$$J(x,\mu) = \begin{bmatrix} 0 & \omega L & -\mu_d \\ -\omega L & 0 & -\mu_q \\ \mu_d & \mu_q & 0 \end{bmatrix}, \quad R(x) = \begin{bmatrix} r & 0 & 0 \\ 0 & r & 0 \\ 0 & 0 & \frac{1}{R_L} \end{bmatrix}, \quad g(x) = \begin{bmatrix} 1 & 0 \\ 0 & 1 \\ 0 & 0 \end{bmatrix} \tag{5}$$

3. The Control of Three-Phase Boost Rectifier.

3.1. The control principle of the system. The final design objective of the PCH system (1) is to find a feedback control $\mu = \beta(x)$ so that the closed-loop dynamics is a state error PCH system with dissipation.

Theorem 3.1. *For the PCH system (1), given $H(x)$, $J(x,\mu)$, $R(x)$ and $g(x)$, let x_0 be a desired equilibrium point, $\tilde{x} = x - x_0$ be the state error, and $\tilde{\mu} = \mu - \mu_0$ be the duty ratio error function. If we can find $H_d(\tilde{x})$, $\beta(x)$, J_a and R_a, satisfying*

$$H_d(0) = 0, \quad H_d(\tilde{x}) > 0 \quad (\forall \tilde{x} \neq 0) \tag{6}$$

$$J_d(\tilde{x},\tilde{\mu}) = J(\tilde{x},\tilde{\mu}) + J_a = -J_d^T(\tilde{x},\tilde{\mu}), \quad R_d(\tilde{x}) = R(\tilde{x}) + R_a = R_d^T(\tilde{x}) > 0 \tag{7}$$

$$\mu = \beta(x) \tag{8}$$

and the closed-loop PCH system (1) with $\mu = \beta(x)$ takes the state error PCH form

$$\dot{\tilde{x}} = [J_d(\tilde{x},\tilde{\mu}) - R_d(\tilde{x})] \frac{\partial H_d(\tilde{x})}{\partial \tilde{x}} \tag{9}$$

Then, $\tilde{x} = 0$ is asymptotically stable equilibrium point of the closed-loop system (9), and the state x does converge to the desired equilibrium x_0 as t tends to infinity.

Proof: From (7), the following expressions are obtained

$$\left[\frac{\partial H_d(\tilde{x})}{\partial \tilde{x}}\right]^T J_d(\tilde{x},\tilde{\mu}) \frac{\partial H_d(\tilde{x})}{\partial \tilde{x}} = 0 \tag{10}$$

Along with the trajectories of the system (9), the time derivative of $H_d(\tilde{x})$ is

$$\frac{dH_d(\tilde{x})}{dt} = \left[\frac{\partial H_d(\tilde{x})}{\partial \tilde{x}}\right]^T \dot{\tilde{x}} = -\left[\frac{\partial H_d(\tilde{x})}{\partial \tilde{x}}\right]^T R_d(\tilde{x}) \frac{\partial H_d(\tilde{x})}{\partial \tilde{x}} < 0 \tag{11}$$

Therefore, the system (9) is asymptotically stable at equilibrium point $\tilde{x} = 0$, and the state x does converge to the desired equilibrium x_0, as t tends to infinity.

Theorem 3.2. *For the system of Theorem 3.1 in closed-loop system with $\mu = \beta(x)$. If*

$$J(\tilde{x} + x_0, \tilde{\mu} + \mu_0) = J(\tilde{x},\tilde{\mu}) + J(x_0,\mu_0) - J(0,0) \tag{12}$$

$$H(x) = \frac{1}{2}x^T D^{-1} x, \quad H_d(\tilde{x}) = \frac{1}{2}\tilde{x}^T D^{-1}\tilde{x} \tag{13}$$

and feedback control $\mu = \beta(x)$ satisfying

$$g(x)u = [J_a - R_a - J(x_0,\mu_0) + J(0,0)]\, D^{-1}\tilde{x} - [J(\tilde{x},\tilde{\mu}) - J(0,0)]\, D^{-1}x_0 + g(x_0)u_0 \tag{14}$$

Then, the closed-loop system can be expressed as the form of Equation (9).

Proof: Since $\tilde{x} = x - x_0$. Thus, $x = \tilde{x} + x_0$. Substituting into (1), we get

$$\begin{aligned} \dot{\tilde{x}} = \dot{x} - \dot{x}_0 = {} & [J(\tilde{x},\tilde{\mu}) + J(x_0,\mu_0) - J(0,0) - R]\, D^{-1}\tilde{x} \\ & + [J(\tilde{x},\tilde{\mu}) - J(0,0)]\, D^{-1}x_0 + g(x)u - g(x_0)u_0 \end{aligned} \tag{15}$$

Let

$$\begin{aligned} \psi = {} & -[J_a - R_a - J(x_0,\mu_0) + J(0,0)]\, D^{-1}\tilde{x} \\ & + [J(\tilde{x},\tilde{\mu}) - J(0,0)]\, D^{-1}x_0 + g(x)u - g(x_0)u_0 \end{aligned} \tag{16}$$

Then, Equation (15) can be written as

$$\dot{\tilde{x}} = [J_d(\tilde{x},\tilde{\mu}) - R_d(\tilde{x})] \frac{\partial H_d(\tilde{x})}{\partial \tilde{x}} + \psi \tag{17}$$

Obviously, Equation (14) ensures that $\psi = 0$, and Equation (9) holds.

3.2. **Controller design.** The control objectives of the three-phase PWM rectifiers are as follows: (i) The output DC voltage tracking control, and $V_{dc} > \sqrt{\frac{3}{2}}E_m$; (ii) The unity power factor regulation, namely, $i_{q0} = 0$.

At steady state, $x_1 = x_{10} = Li_{d0}$, $x_2 = 0$, $x_3 = x_{30} = CV_{dc}$. According to (2) and $i_{q0} = 0$, i_{d0} can be calculated

$$\begin{cases} \sqrt{\frac{3}{2}}E_m - ri_{d0} - \mu_{d0}V_{dc} = 0 \\ \omega Li_{d0} + \mu_{q0}V_{dc} = 0 \\ \mu_{d0}i_{d0} - \frac{V_{dc}}{R_L} = 0 \end{cases} \tag{18}$$

$$i_{d0} = \frac{1}{2}\left(\frac{\sqrt{\frac{3}{2}}E_m}{r} - \sqrt{\frac{3E_m^2}{2r^2} - \frac{4V_{dc}^2}{rR_L}}\right), \quad \mu_{d0} = \frac{\sqrt{\frac{3}{2}}E_m - ri_{d0}}{V_{dc}}, \quad \mu_{q0} = -\frac{\omega Li_{d0}}{V_{dc}} \tag{19}$$

$$x_0 = \begin{bmatrix} x_{10} & x_{20} & x_{30} \end{bmatrix}^T = \begin{bmatrix} Li_{d0} & 0 & CV_{dc} \end{bmatrix}^T \tag{20}$$

The desired Hamiltonian function of closed-loop system is given by

$$H_d(\tilde{x}) = \frac{1}{2}(x - x_0)^T D^{-1}(x - x_0) \tag{21}$$

$$J_a = \begin{bmatrix} 0 & j_{a12} & j_{a13} \\ -j_{a12} & 0 & j_{a23} \\ -j_{a13} & -j_{a23} & 0 \end{bmatrix}, \quad R_a = \begin{bmatrix} r_{a1} & 0 & 0 \\ 0 & r_{a2} & 0 \\ 0 & 0 & r_{a3} \end{bmatrix} \tag{22}$$

Since $g(x)u$ is a constant and $g(x)u = g(x_0)u_0$, according to (14) we obtain

$$[J_a - R_a - J(x_0, \mu_0) + J(0,0)]D^{-1}\tilde{x} - [J(\tilde{x}, \tilde{\mu}) - J(0,0)]D^{-1}x_0 = 0 \tag{23}$$

Then, the controller equations are

$$\mu_d = \mu_{d0} + \frac{1}{V_{dc}}[r_{a1}(i_d - i_{d0}) - (j_{a12} - \omega L)i_q - (j_{a13} + \mu_{d0})(u_{dc} - V_{dc})] \tag{24}$$

$$\mu_q = \mu_{q0} + \frac{1}{V_{dc}}[(j_{a12} - \omega L)(i_d - i_{d0}) + r_{a2}i_q - (j_{a23} + \mu_{q0})(u_{dc} - V_{dc})] \tag{25}$$

and the assignment equation is

$$(\mu_d - \mu_{d0})i_{d0} = -(j_{a13} + \mu_{d0})(i_d - i_{d0}) - (j_{a23} + \mu_{q0})i_q - r_{a3}(u_{dc} - V_{dc}) \tag{26}$$

Substituting (19) and (24) into (26), we get

$$\begin{aligned} &(j_{a23}V_{dc} - j_{a12}i_{d0})i_q + r_{a1}i_{d0}(i_d - i_{d0}) + r_{a3}V_{dc}(u_{dc} - V_{dc}) \\ &+(j_{a13} + \mu_{d0})(i_dV_{dc} - i_{d0}u_{dc}) = 0 \end{aligned} \tag{27}$$

To make Equation (27) always hold, parameters are matched as follows

$$j_{a23} = j_a i_{d0}, \quad j_{a12} = j_a V_{dc}, \quad r_{a1} = r_{a3} = 0, \quad j_{a13} = -\mu_{d0}$$

where j_a is interconnection parameter, and r_{a2} is positive damping parameter.

Consequently, from (24) and (25) we obtain the control laws

$$\begin{cases} \mu_d = \frac{1}{V_{dc}}\left[\sqrt{\frac{3}{2}}E_m - ri_{d0} - (j_aV_{dc} - \omega L)\,i_q\right] \\ \mu_q = \frac{1}{V_{dc}}\left[-\omega Li_{d0} + (j_aV_{dc} - \omega L)(i_d - i_{d0}) + r_{a2}i_q - i_{d0}\left(j_a - \frac{\omega L}{V_{dc}}\right)(u_{dc} - V_{dc})\right] \end{cases} \tag{28}$$

3.3. **The PI regulation of output DC voltage error.** The parasitic elements and parameter inaccuracies may lead to an incorrect i_{d0} and cause steady-state error of output DC voltage. Therefore, the PI control is used to eliminate the steady-state error of output DC voltage. Assume new equilibrium is taken as i_{d0}^*, that is

$$i_{d0}^* = i_{d0} + \Delta i_{d0}, \quad \Delta i_{d0} = -k_p(u_{dc} - V_{dc}) - k_i \int_0^t (u_{dc} - V_{dc})dt \tag{29}$$

The control laws with PI regulation can be expressed as

$$\begin{cases} \mu_{di} = \frac{1}{V_{dc}}\left[\sqrt{\frac{3}{2}}E_m - ri_{d0}^* - (j_a V_{dc} - \omega L)i_q\right] \\ \mu_{qi} = \frac{1}{V_{dc}}\left[-\omega L i_{d0}^* + (j_a V_{dc} - \omega L)(i_d - i_{d0}^*) + r_{a2} i_q - i_{d0}^*\left(j_a - \frac{\omega L}{V_{dc}}\right)(u_{dc} - V_{dc})\right] \end{cases} \tag{30}$$

3.4. **The SVPWM implementation of the controller.** The SVPWM needs reference voltage vector component in $\alpha\beta$ coordinates.

$$\nu_{di} = \mu_{di} u_{dc}, \quad \nu_{qi} = \mu_{qi} u_{dc} \tag{31}$$

In Figure 1, ν_{di} and ν_{qi} are values of ν_a, ν_b and ν_c in the d-q frame respectively. Then, we get

$$\begin{bmatrix} u_\alpha \\ u_\beta \end{bmatrix} = \begin{bmatrix} \cos\omega t & -\sin\omega t \\ \sin\omega t & \cos\omega t \end{bmatrix} \begin{bmatrix} \nu_{di} \\ \nu_{qi} \end{bmatrix} \tag{32}$$

Therefore, the pulse signals which drive six IGBT switches can be generated by SVPWM signal transformation.

4. **The Comparative Studies and Simulation Experiment Results.** The circuit parameters: $E_m = 80$V, $f = 50$Hz, $L = 15$mH, $r = 1\Omega$, $C = 2200\mu$F, $R_L = 80\Omega$, $V_{dc} = 200$V. The controller parameters: $j_a = 1$, $r_{a2} = 50$, $k_p = 0.8$, $k_i = 0.03$.

Figure 2 shows the waveform of the output DC voltage under the PCH control with PI regulation. At $t = 0.125$s, the load resistance changes from 80Ω to 40Ω. The output voltage steady-state error is eliminated quickly. Figure 3 shows the waveforms of u_a and i_a. The i_a is not only sinusoidal wave, but also the same phase as the u_a.

Figure 4 gives the waveform of the output DC voltage. At $t = 0.125$s, V_{dc} changes from 200V to 150V. The actual voltage tracks V_{dc} rapidly without steady-state error. Figure 5 shows the waveforms of u_a and i_a. At steady-state, the i_a is the same phase as the u_a.

The existing VOC is a classical control method [2]. In order to compare the proposed control algorithm and the VOC, the VOC simulation experiments have been carried out.

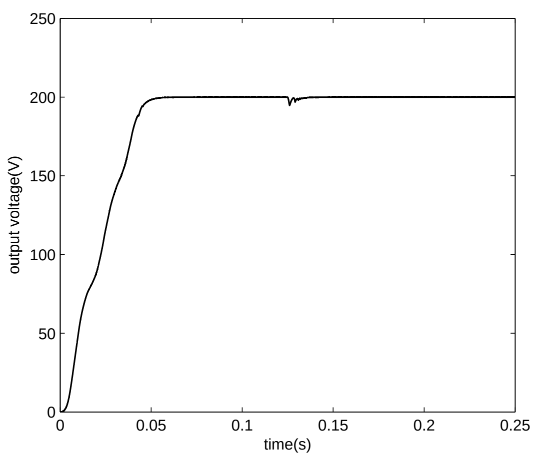

FIGURE 2. Curve of u_{dc} when the load changes

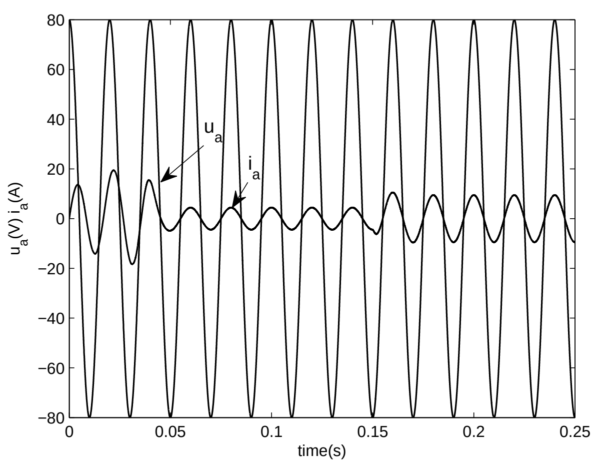

FIGURE 3. Curves of u_a and i_a when the load changes

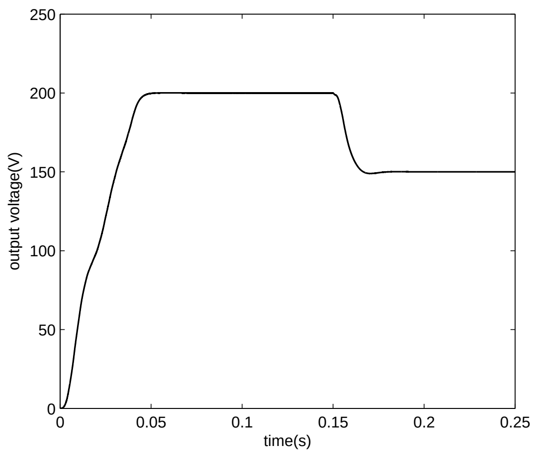

FIGURE 4. Curve of u_{dc} when V_{dc} changes

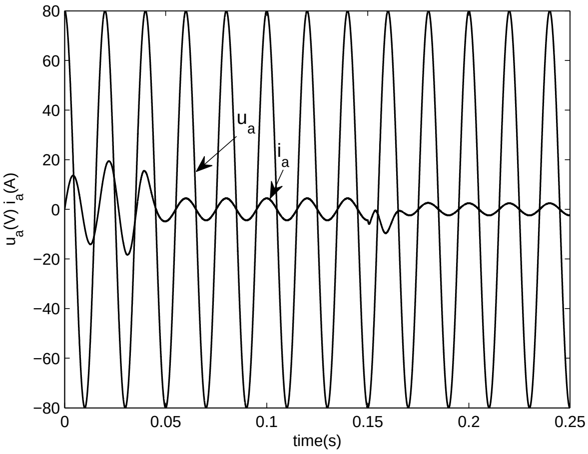

FIGURE 5. Curves of u_a and i_a when V_{dc} changes

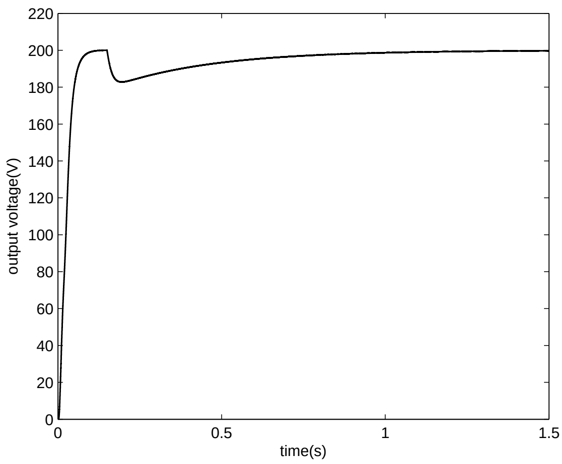

FIGURE 6. The u_{dc} curve of VOC when load changes

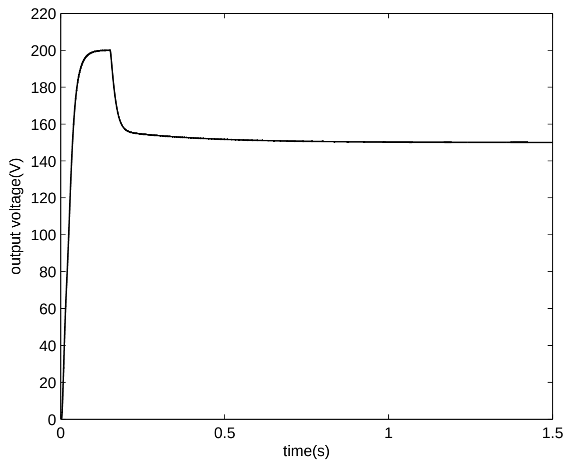

FIGURE 7. The u_{dc} curve of VOC when V_{dc} changes

The parameters of two PI regulators are $k_{ip} = 3$, $k_{ii} = 1.1$; $k_{vp} = 0.25$, $k_{vi} = 0.15$. Figure 6 shows that transient process of output DC voltage is longer when load resistance changes from 80Ω to 40Ω at $t = 0.15$s. Moreover, Figure 7 shows that the output DC voltage response of the VOC is very slow when V_{dc} changes from 200V to 150V at $t = 0.15$s.

5. **Conclusion.** In this paper, the high performance control of three-phase boost rectifier is presented based on the state error PCH control and the energy-shaping principle. The PCH system model is established for the PWM rectifier. The desired state error PCH system structure is assigned to closed-loop control system. The controller design problem is reduced to the solution of a set of partial differential equations. Although the solving of the PDE is very difficult, we can transform the PDE into a set of ordinary differential equation through energy-shaping and interconnection assignment and damping injection. Moreover, the PI regulation is added to eliminate the steady-state error of the output DC voltage. The proposed control algorithm has good output voltage tracking control and unity power factor regulation performances. The further potential study trend is the load disturbance attenuation and parameters adaptive control.

Acknowledgment. This work is supported by the National Natural Science Foundation of China (61573203, 61573204), Shandong Province Outstanding Youth Fund (ZR2015JL0 22).

REFERENCES

[1] H. Yu, Z. Teng, J. Yu and Y. Zang, Energy-shaping and passivity-based control of three-phase PWM rectifiers, *The 10th World Congress on Intelligent Control and Automation*, Beijing, China, pp.2844-2848, 2012.

[2] J. Dannehl, C. Wessels and F. W. Fuchs, Limitations of voltage-oriented PI current control of grid-connected PWM converters with filters, *IEEE Trans. Industrial Electronics*, vol.56, no.2, pp.380-388, 2009.

[3] M. P. Kazmierkowski and L. Malesani, Current control techniques for three-phase voltage-source PWM converters: A survey, *IEEE Trans. Industrial Electronics*, vol.45, no.5, pp.691-703, 1998.

[4] S. Kwak and J. C. Park, Model predictive direct power control with vector preselection technique for highly efficient active rectifiers, *IEEE Trans. Industrial Informatics*, vol.11, no.1, pp.44-52, 2015.

[5] Z. Zhou and Y. Liu, Pre-sampled data based prediction control for active power filters, *International Journal of Electrical Power and Energy System*, vol.37, no.1, pp.13-22, 2012.

[6] A. Luo, L. Fang, X. Xu, S. Peng, C. Wua and H. Fang, New control strategy for DSTATCOM without current sensors and its engineering application, *International Journal of Electrical Power and Energy System*, vol.33, no.2, pp.322-331, 2011.

[7] C. Albea and F. Gordillo, Adaptive control design for a boost inverter, *Control Engineering Practice*, vol.19, no.1, pp.32-44, 2011.

[8] R. Ortega, A. J. vander Schaft and B. Maschke, Interconnection and damping assignment passivity-based control of port-controlled hamiltonian systems, *Automatica*, vol.38, no.4, pp.585-596, 2002.

[9] A. Macchelli, Passivity-based control of implicit port-hamiltonian system, *SIAM Journal on Control and Optimization*, vol.52, no.4, pp.2422-2448, 2014.

[10] H. Yu, J. Yu, J. Liu and Y. Wang, Energy-shaping and L_2 gain disturbance attenuation control of induction motor, *International Journal of Innovative Computing, Information and Control*, vol.8, no.7(B), pp.5011-5024, 2012.

[11] J. Chi, H. Yu and J. Yu, Hybrid control of PMSM based on signal and energy, *ICIC Express Letters, Part B: Applications*, vol.6, no.1, pp.193-199, 2015.

[12] H. Yu, J. Yu and J. Liu, Nonlinear control of induction motors based on state error PCH and energy-shaping principle, *Nonlinear Dynamics*, vol.72, no.1, pp.49-59, 2013.